Strong Akaganeite Aerogel Monoliths Using Epoxides: Synthesis and Characterization

Alexander E. Gash,*[,†,‡] Joe H. Satcher, Jr.,[†] and Randall L. Simpson[†,‡]

Chemistry and Materials Science Directorate and Energetic Materials Center, Lawrence Livermore National Laboratory, Livermore, California 94551

Received March 28, 2003. Revised Manuscript Received June 17, 2003

The synthesis of iron(III) oxide aerogel monoliths was performed by adding any one of several different 1,2- and 1,3-epoxides to ethanolic Fe(III) salt solutions at room temperature. While all of the epoxides examined resulted in gel formation, robust low-density (∼30−40 kg/m^3; 99% porous), high-surface-area (∼250−300 m^2/g), aerogel monoliths were prepared by the addition of 1,3-epoxide derivatives to solutions of $FeCl_3 \cdot 6H_2O$, followed by drying with supercritical CO_2. Both types of iron(III) oxide aerogels (those made with 1,2- and 1,3-epoxides respectively) were characterized using elemental analysis, X-ray diffraction, thermal analysis, acoustic measurements, transmission electron microscopy, scanning electron microscopy, and N_2 adsorption desorption analysis. Elemental analyses and powder X-ray diffraction indicated that the strong aerogel monoliths made with the 1,3-epoxides are made up predominately of polycrystalline β-FeOOH, akaganeite, and those made with the 1,2-epoxides are amorphous. To our knowledge, this is first known report of synthesis and characterization of akaganeite aerogel materials. Transmission electron microscopy analysis indicates that aerogels derived using 1,3-epoxides have a microstructure made up of a highly reticulated network of fibers with diameters from ∼5 to 35 nm and lengths several times that, whereas those resulting from the use of 1,2-epoxides consist of interconnected spherical particles, whose diameters are 5−15 nm. The difference in microstructure results in each type of aerogel displaying very distinct physical and mechanical properties. In particular, the stiffness of the β-FeOOH aerogels is remarkable for a transition metal oxide aerogel. Monolithic cylinders of β-FeOOH aerogel can be sintered at 515 °C, transforming to α-Fe_2O_3 without shattering.

Introduction

The mineral name of β-FeOOH, akaganeite, is derived from the Akagané mine in Japan where it was first reported.[1] It is a brownish-yellow solid that typically forms in powdery masses in the environment. The mineral is a component of soils and geothermal brines as well as a corrosion product of both steel and iron-bearing meteorites.[2] Akaganeite has been studied and utilized as a catalyst, pigment, and size-selective anion-exchange material.[2,3] It forms in the environment in the presence of chloride ions at elevated temperatures and can be prepared synthetically by the slow hydrolysis of $FeCl_3$ solutions at low pH with heating to 70−100 °C.

The structure of akaganeite consists of double chains of edge-sharing octahedra that share corners with adjacent chains to form channels that run parallel to the crystallographic *b*-axis.[4] The channels are stabilized with residual chloride ions and water molecules. The chloride anions are present to charge balance excess protons present on the iron oxide framework as the synthesis of akaganeite proceeds only at low pH. This tunnel structure makes β-FeOOH an especially interesting material in the areas of catalysis and ion exchange.[5−7] For example, akaganeite is a size-selective inorganic ion-exchange material, possessing both tunnel and surface exchange sites. Larger anions such as perchlorate can only attach at surface sites, whereas smaller anions such as F^- can fit in the tunnels.[5,6] Akaganeite crystals display two typical morphologies: somatoids or cigar-shaped crystals or smaller rodlike crystals.

Aerogels have several distinct and uncommon properties that make them attractive for technical applications in many areas.[8−11] They possess high porosity (90−99%), high surface area, low density, some degree of optical

* Corresponding author. Phone: (925)423-8618. Fax: (925)423-4897. E-mail: gash2@llnl.gov.
† Chemistry and Materials Science Directorate.
‡ Energetic Materials Center.

(1) Mackay, A. L. *Miner. Magn.* **1962**, *33*, 270.
(2) Cornell, R. M.; Schwetmann, U. *The Iron Oxides*; VCH Publishers: Weinheim, 1996.
(3) Schwetmann, U.; Cornell, R. M. *Iron Oxides in the Laboratory*; VCH Publishers: New York, 1991.
(4) Post, J. E.; Buchwald V. F. *Am. Miner.* **1991**, *76*, 272.
(5) Patterson, R.; Rahman, H. *J. Colloid Interface Sci.* **1983**, *94* (1), 60.
(6) Patterson, R.; Rahman, H. *J. Colloid Interface Sci.* **1983**, *97* (2), 423.
(7) Pradel, J.; Castillo, S.; Traverse, J.-P. *Ind. Chem. Res.* **1993**, *32*, 1801.
(8) Hüsing, N.; Schubert U. *Angew. Chem., Int. Ed.* **1998**, *37*, 22.
(9) Pierre, A. C.; Pajonk, G. M. *Chem. Rev.* **2002**, *102*, 4243.
(10) Baumann, T. F.; Gash, A. E.; Fox, G. A.; Satcher, J. H., Jr.; Hrubesh, L. W. In *Handbook of Porous Solids*; Schüth, F., Sing, K. S., Weitkamp, J., Eds.; Wiley-VCH: Weinheim, 2002; Vol. 3, pp 2014−2037.
(11) Hrubesh, L. W. *J. Non-Cryst. Solids* **1998**, *225*, 335.

10.1021/cm034211p CCC: $25.00
Published on Web 07/23/2003

Chart 1. (a) 1,2-Epoxide and (b) 1,3-Epoxide Structures

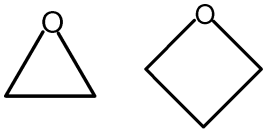

a) b)

transparency, and low thermal conductivity. Their unique properties are a result of their unusual microstructure, which consists of a continuous network of colloidal particles, or polymeric chains with characteristic diameters of ~10 nm, open porosity, and characteristic pore diameters less than 100 nm. Aerogels have been studied for application as thermal insulators, catalysts, dielectrics, optical coatings, laser targets, waste remediation materials, sensors, pesticides, energetic materials, and collectors for high-energy particles.[10]

Although they are technologically fascinating, aerogels have limitations. In addition to the cost of supercritical processing, one must take into account synthetic routes, the final form of the material, and how it functions in each application. With this in mind, aerogels are fragile materials that are easily damaged upon handling. Many aerogels are supercritically dried to aerogel powders or highly cracked and fragile monoliths that cannot be handled without severe restrictions.[9] This limits their utility in areas where processing or application dictates some structural form with moderate strength (e.g., laser target components).[11] An exception here are SiO_2 aerogels, which can be dried to monoliths without cracking and can be handled reasonably without damage. This property has helped to facilitate the application of silica and doped silica aerogels in many of the above-mentioned areas. The synthesis of strong, monolithic, stable, non-silica aerogels has been found to be especially difficult. Therefore, the synthesis of robust aerogels with greater chemical range and variety would be of interest to future aerogel application studies.

We have reported on the use of 1,2-epoxides as gelation agents for the synthesis of iron(III) oxide aerogels and xerogels from Fe(III) inorganic salt precursors.[12,13] The 1,2-epoxides have at least one three-member cyclic ether ring in their structure (see Chart 1a). Different substituents, at the positon(s) α to the oxygen, can strongly affect the epoxide's reactivity through steric or electronic effects, or both. The 1,3-epoxides have a four-member cyclic ether ring in their structure (see Chart 1b). Both 1,2- and 1,3-epoxides undergo the same types of ring-opening reactions. However, the 1,3-epoxides undergo these reactions much less readily than the 1,2-epoxides.[14]

This publication details the influence that the type of epoxide employed has on the microstructure and properties of the resulting iron(III) oxide aerogel. Both 1,2-epoxide and 1,3-epoxide derivatives were used as gelation agents for the preparation of monolithic iron(III) oxide aerogels. The microstructural, chemical, and mechanical properties of the resulting aerogels strongly depend on the type of epoxide used. Akaganeite aerogels with 99% porosity were prepared as surprisingly stiff monoliths from iron(III) chloride solutions using 1,3-epoxides. To our knowledge, this is the first report of the synthesis and characterization of such aerogel materials. It also provides a new room-temperature synthetic approach to akaganeite. The β-FeOOH aerogels have remarkably good mechanical properties, given their low densities, when compared to other iron(III) oxide aerogels made with 1,2-epoxides, and with SiO_2, and Al_2O_3 aerogels with similar densities. The choice of epoxide used also provides fine control over the levels of meso- and macroporosity in the dry aerogels.

Experimental Section

Synthesis of Iron(III) Oxide Aerogels. The iron(III) salt used was $FeCl_3 \cdot 6H_2O$. Epoxides used as gelation agents here included propylene oxide (PO), *cis*-2,3-epoxybutane, 1,2-epoxybutane, glycidol, epichlorohydrin, epibromohydrin, epifluorohydrin, 3,3,-dimethyloxetane (DMO), and trimethylene oxide (TMO). All reactants were reagent grade or better obtained from Aldrich Chemical Co. and were used as received. The ethanol used was 200 proof from Aaper. A typical gel synthesis experiment went as follows: 0.42 g (1.6 mmol) of $FeCl_3 \cdot 6H_2O$ was dissolved in 3.5 mL of ethanol to give a clear yellow/orange solution. To that solution 0.1 g (5.5 mmol) of distilled H_2O was added followed by the immediate addition of an appropriate amount of epoxide (16 mmol) to give a epoxide/Fe ratio of ~10. In most experiments, the requisite amount of epoxide was added in one step; however, in some, the prescribed portion epoxide was added in small incremental amounts over a period of many hours. For example, in one experiment PO was added to a 0.41 M $FeCl_3 \cdot 6H_2O$ ethanol solution in 0.02-mL increments over a 20-h period.

After the addition of the epoxide, the solution changed from a clear orange/yellow to an intense dark reddish-brown or a yellowish-brown (depending on the epoxide used), and some point after the addition, a rigid wet gel of the same color formed. The time from epoxide addition to gelation for each synthesis experiment is related to the reactivity of the individual epoxide and varied from a few minutes to a few days. (**Caution:** with the use of some epoxides (specifically, propylene oxide) the color change is accompanied by significant heat generation, which in some cases led to rapid boil over of the synthesis solution. We recommend the cautious addition of the epoxide to the Fe(III) solution in a well-ventilated laboratory space.)

Processing of Iron(III) Oxide Gels. The wet gels were covered and allowed to age for at least 24 h under ambient conditions. After that they were immersed in a bath of absolute ethanol where they were washed for ~1 week. Aerogel samples were processed in Polaron supercritical point drier. The solvent liquid in the wet gel pores was exchanged for CO_2 (l) for 2−3 days, after which the temperature of the vessel was ramped up to ~45 °C, while a pressure of ~100 bar was maintained. The vessel was then depressurized at a rate of ~7 bar/h. All of the dry aerogels were reddish-brown with the exception of the DMO-derived gels, which were yellowish-brown.

A β-FeOOH aerogel monolith was subjected to prolonged heating, under inert atmosphere, and still retained its monolithic form. In this experiment, a monolith was heated to 300 °C at 5 °C/min., in a furnace, under a N_2 flow, and held at that temperature for 3 h before turning off the furnace and cooling to 50 °C. This process was repeated on the same sample at 325, 415, and finally 515 °C to yield a bright red α-Fe_2O_3 aerogel (ρ = 770 kg/m^3 (85% porous)) monolith.

(12) Gash, A. E.; Tillotson, T. M.; Satcher, J. H., Jr.; Poco, J. F.; Hrubesh, L. W.; Simpson, R. L. *Chem. Mater.* **2001**, *13*, 999.
(13) Gash, A. E.; Tillotson, T. M.; Satcher, J. H., Jr.; Hrubesh, L. W.; Simpson, R. L. *J. Non-Cryst. Solids* **2001**, *285*, 22.
(14) Dobinson, B.; Hofmann, W.; Stark, B. P. *The Determination of Epoxide Groups*; Permagon Press: Oxford, 1969.

Table 1. Summary of Gel Times for Iron(III) Oxide Gels Made with Different Epoxides[a]

epoxide	t_{gel} (min)
1,2-epoxides	
cis-2,3-epoxybutane	2.8
propylene oxide	7
1,2-epoxybutane	12
glycidol	16
epichlorohydrin	20
epifluorohydrin	18
epibromohydrin	25
1,3-epoxides	
trimethylene oxide	8−24 h
3,3-dimethyloxetane	48−72 h

[a] Conditions of syntheses: precursor salt $FeCl_3 \cdot 6H_2O$, solvent ethanol, [Fe] = 0.41 M, H_2O/Fe(III) = 11, and epoxide/Fe = 10.

Physical Characterization. Surface area and pore volume and size analyses were performed using an ASAP 2000 surface area analyzer (Micromeritics Instrument Corp.) with resulting data analyzed by Brunauer−Emmett−Teller (BET) and Barrett−Joyner−Halenda (BJH) methods. Samples of aerogel (0.1−0.2 g) were heated to 200 °C under vacuum (10^{-5} Torr) for at least 24 h to remove all adsorbed species. Nitrogen adsorption data were taken at five relative pressures from 0.05 to 0.20 at 77 K, to calculate the surface area by BET theory. All nitrogen adsorption/desorption measurements were required to equilibrate for a minimum of 40 s before being recorded. Typical nitrogen adsorption/desorption experiments took 20−50 h to complete. For the BJH analyses, average pore size and pore volume were calculated using the data points from the desorption branch of the isotherm.

The high-resolution transmission electron microscopy (HRTEM) was performed on a Philips CM300FEG operating at 300 keV using zero loss energy filtering with a Gatan energy imaging filter (GIF) to remove inelastic scattering. The images were taken under bright field conditions and slightly defocused to increase contrast. The images were also recorded on a 2K × 2K CCD camera attached to the GIF. Powdered samples were dispersed in methanol, and drops of the resulting mixture were deposited onto a carbon-coated Cu grid using a pipet.

Scanning electron microscopy (SEM) was carried out using a Hitachi S-4500 cold field emission SEM. Typical accelerating voltages used for aerogel samples ranged from 1.8 to 6 kV and depended on sample conductivity. No sample preparation (i.e., coating with conductive layer of Au) was performed on the samples. Powder X-ray diffraction data were collected on aerogel samples using an APD3720 PEI automatic powder diffractometer with an analyzing crystal. Cu Kα radiation was used. Samples were mounted on an aluminum plate. Elemental analyses of aerogel samples were performed by Galbraith Laboratories, Inc. of Knoxville, TN.

The elastic moduli of the iron(III) oxide aerogels were calculated using the measured densities and longitudinal and shear sound velocities, according to the procedures reported by Gross et al.[15] Sound velocity measurements were made with a Panametrics ultrasonic analyzer model 5052UA with 180-kHz center frequency transducers. Measurements were made on monolithic right circular cylinders of aerogel with flat smooth parallel surfaces and lengths between 0.6 and 2.0 cm.

Results

Synthesis. The synthesis of iron(III) oxide gels using a variety of different epoxides was performed, the results of which are summarized in Table 1. A number of commercially available 1,2- and 1,3-epoxides were evaluated. All of the epoxides listed were capable of inducing iron(III) oxide gel formation. According to Table 1, the times for gel formation do not vary appreciably for all of the syntheses that use 1,2-epoxide derivatives. However, the gel times when 1,3-epoxides (TMO, DMO) are used are markedly longer than those using the three member epoxide derivatives. We believe that the large difference in gel times for the above materials can be directly correlated to the relative reactivity of the respective epoxide. The 1,2-epoxides are more strained and, therefore, more reactive than the 1,3-epoxides to ring-opening reactions.[14] For example, PO acts to raise the pH of the Fe^{3+} solution more rapidly than DMO, hence, the more rapid gelation.

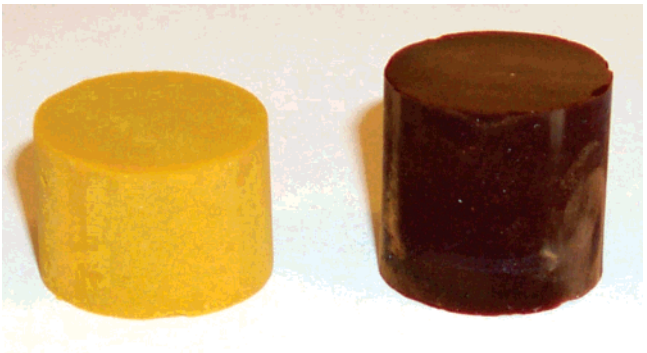

Figure 1. Photo of two β-FeOOH aerogels made with 1,3-epoxides, one using DMO (yellow aerogel) and one made using TMO as the gelation agent (reddish-brown aerogel). Both aerogels have ρ = 40 kg/m^3 and diameters of ∼1.5 cm.

All of the gels summarized in Table 1 were processed to aerogels by exchange of the pore liquid with CO_2(l) followed by supercritical drying. The physical appearances of the resulting aerogels were quite different. Aerogels made with the 1,2-epoxides are reddish-brown, somewhat transparent, undergo significant shrinkage (50−70%), and as a result are often cracked and have densities ranging from 70 to 200 kg/m^3. In many cases, these aerogels come out of the supercritical extraction process as powders. Alternatively, the 1,3-epoxide-derived aerogels display relatively little shrinkage (5−15%), are rarely cracked, have low densities (30−40 kg/m^3), and are much stiffer than the aerogels made with 1,2-epoxides. Figure 1 is a photograph of two aerogels made with 1,3-epoxides. Aerogels made with DMO are yellowish-brown monoliths, whereas those derived using TMO are reddish-brown. The materials are transparent, as their ultrafine cell/pore size(s) minimize light scattering in the visible spectrum, and highly colored.

Electron Microscopy. TEM was used to evaluate the microstructure of the aerogels reported here. Figures 2−4 contain micrographs of PO-, DMO-, and TMO-derived aerogels, respectively. Inspection of Figure 2 indicates that the PO-derived aerogel is made up of interconnected spherical particles. The particles are 5−15 nm in diameter, and they are amorphous to X-ray and electron diffraction. This type of microstructure is typical of many main group and transition metal aerogels and is best described as "colloidal-like".[16]

The microstructure of the DMO-derived aerogel is shown in Figure 3. The material appears to be much less dense and more highly interconnected than the propylene oxide-derived aerogel. The morphology of the DMO-derived gel is fibrous as opposed to particulate.

(15) Gross, J.; Reichenauer, G.; Fricke, J. *J. Phys. D* **1988**, *21*, 1447.

(16) Brinker, C. J.; Scherer, G. W. *Sol−Gel Science*; Academic Press: Boston, 1990.

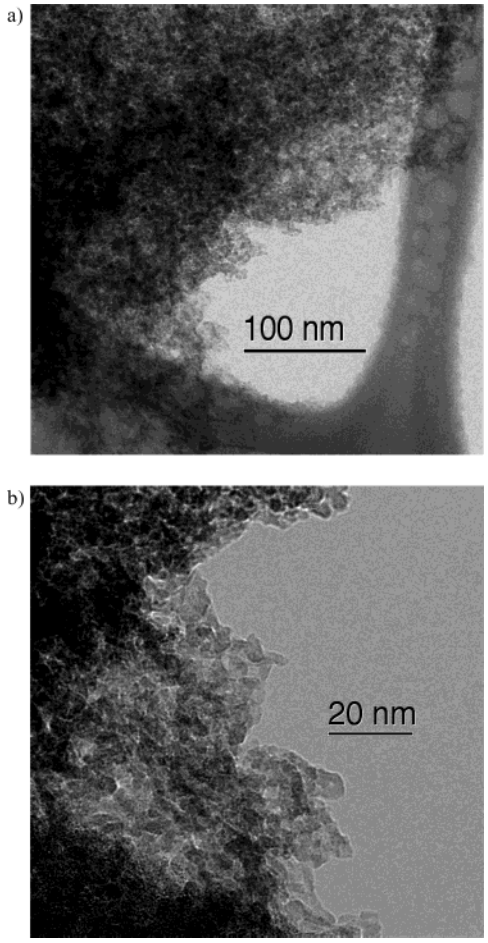

Figure 2. TEM images of an iron(III) oxide aerogel made with $FeCl_3 \cdot 6H_2O$ using PO as the gelation agent.

The aerogel shown in Figure 3 is made up of fiberlike particles that are approximately 15−35 nm in diameter, of varying length, and reticulated to form a highly interconnected microstructure. In fact, it is difficult to determine the actual length of the particles from the TEM images because many of the ribbons are either entangled or continue out of the field of view of the image. Nonetheless, one can see that the length of these particles is many times that of the width. Aerogels of sol−gel acid-catalyzed SiO_2 and V_2O_5 with similar morphologies have been reported and are often referred to as "polymeric-like".[16,17]

Figure 4 is a HRTEM image of the TMO-derived gel and is an excellent representation of the morphology of the fibers that make up iron(III) oxide aerogels derived from 1,3-epoxides. However, it appears that the fibers in the TMO-derived aerogels are significantly narrower (∼2−5 nm) than those in the DMO-derived ones (15−35 nm).

The surface morphology of the iron(III) oxide aerogels was evaluated with SEM. Figure 5 contains micrographs of both types of aerogels. Figure 5a,b contains SEM images of an aerogel made with DMO. Figure 5a is a lower magnification image of the aerogel. It indicates that the material is highly porous with a mosslike, highly branched microstructure. The higher magnification image in Figure 5b reinforces this and reveals a

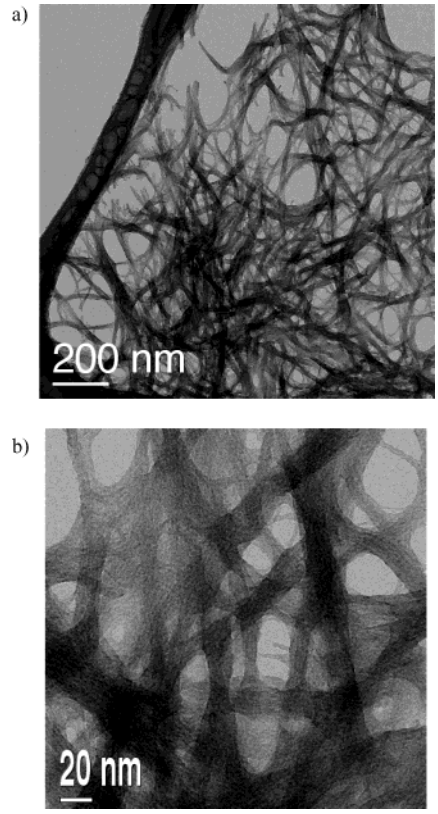

Figure 3. TEM images of an iron(III) oxide aerogel made with DMO as the gelation agent. The thick long fiber in the upper left portion of (a) is a portion of the carbon grid used to hold the sample.

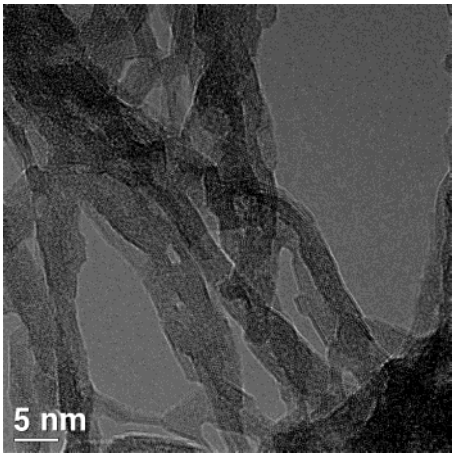

Figure 4. High-resolution transmission electron micrograph of akaganeite aerogel material made with TMO.

morphology that appears to consist of small bundles (∼50 nm in diameter and up to 500 nm in length) of fiberlike particles. Figure 5c is a high-magnification SEM image of iron(III) oxide aerogel made with propylene oxide. This image reveals a porous microstructure made up of small spherically shaped particles that are interconnected.

The aerogels made with 1,3-epoxides are significantly stiffer than those made with 1,2-epoxides. To investigate this observation, sound velocity measurements on right circular cylinders of selected aerogels were taken and the elastic moduli for a series of aerogels were calculated. Since elastic modulus scales with density only aerogels with similar densities should be compared.[18]

(17) Livage, J.; Henry, M. Sanchez, C. *Prog. Solid State Chem.* **1988**, *18*, 259.

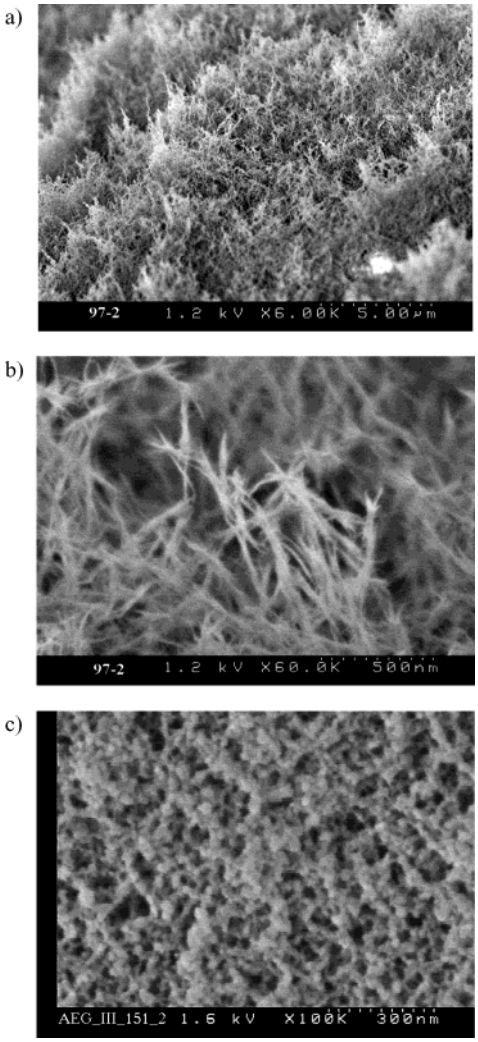

Figure 5. Scanning electron micrographs of iron(III) oxide aerogels made with the 1,3-epoxide DMO (a and b) and with the 1,2-epoxide PO (c).

Table 2. Some Measured Properties of Iron(III) Oxide Aerogels Prepared with Different Epoxides and Other Aerogels

material	epoxide	surf. area BET (m^2/g)	pore vol (mL/g)	av pore diam (nm)	density (kg/m^3)	elastic modulus (MPa)
Fe(III) oxide	PO	345 ± 4	3.88	26	70 ± 4	1.01 ± 0.10
Fe(III) oxide	TMO				71 ± 4	3.71 ± 0.40
Fe(III) oxide	TMO	356 ± 3	5.93	31	40 ± 2	0.67 ± 0.07
Fe(III) oxide	DMO	289 ± 3	0.56	8.1	38 ± 2	0.68 ± 0.07
Al_2O_3[a]					37 ± 2	0.55 ± 0.06
SiO_2[a]					39 ± 2	0.49 ± 0.05

[a] Data taken from ref 16.

Table 2 indicates that the elastic modulus of a PO-derived aerogel (with colloidal-like microstructure) with density of 70 ± 4 kg/m^3 is 1.01 ± 0.10 MPa whereas that for a TMO-derived aerogel (with polymeric-like microstructure) with density of 71 ± 3 kg/m^3 is 3.71 ± 0.40 MPa, nearly a factor of 4 difference. The elastic moduli for DMO- and TMO-derived aerogels with a density of ∼40 kg/m^3 are nearly the same. Finally, the elastic moduli of the 1,3-epoxide-derived aerogels are higher that those for similar density aerogels with different compositions (SiO_2 and Al_2O_3) that have been recently reported.[18]

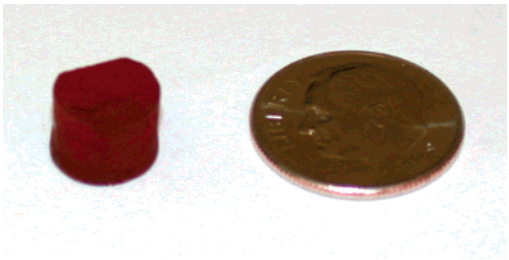

Figure 6. Hematite aerogel monolith (ρ = 770 kg/m^3 (85% porous)) produced by heating an akaganeite aerogel to 515 °C for 3 h.

Elemental Analysis. The PO-derived material contains slightly more carbon (5.2 wt %) and hydrogen (2.6 wt %) than the TMO- (3.2 and 2.5 wt %) and DMO-derived aerogels (3.7 and 2.7 wt %). However, this difference is slight and the low overall values indicate that most of the solvent, epoxide, and epoxide byproducts are effectively removed with the CO_2(l) exchange and supercritical drying. The most significant variation in elemental makeup of the three aerogels is the amount of chloride present. The two aerogels made with TMO and DMO contain 5.98 and 10.99 wt % chloride, respectively, whereas the PO-derived aerogel has 1.34 wt % chloride. These results are very consistent and reproducible with other samples. Akaganeite typically contains between 1 and 7 wt % chloride.[2,3] The calculated chloride stoichiometries (relative to Fe) of the three-aerogel types are $FeOOHCl_{0.04}$, $FeOOHCl_{0.17}$, and $FeOOHCl_{0.38}$, respectively.

Thermal Analysis. Simultaneous thermal gravimetric and differential thermal analyses (TGA/DTA), in a N_2 atmosphere, were performed on the akaganeite aerogel. Although not shown here, the akaganeite aerogel sample begins losing weight without delay as the temperature begins to rise. The mass loss appears to be fairly constant up to ∼400 °C where it ends. The total mass loss was 34 wt %. Iron oxides that contain structural OH groups undergo dehydroxylation from 250 to 400 °C. The DTA portion of the trace indicated only one major thermal feature: an exotherm at ∼290 °C. Akaganeite is known to undergo dehydroxylation and phase transition to give hematite on heating to ∼500 °C.[3] Heating of an aerogel monolith of β-FeOOH to 515 °C under a N_2 purge leads to the formation of a bright red monolith (see Figure 6). There is an extreme volume reduction as the bulk density of the monolith increases from 40 to 770 kg/m^3. The red monolith has been identified as a α-Fe_2O_3, hematite, aerogel. Thus, the aerogel undergoes a phase transformation without destruction of the monolith. The surface area of the sample decreases from 289 to 44 m^2/g upon heat treatment, and the material is still ∼85% porous.

Powder X-ray Diffraction. Aerogels prepared using both the 1,3-epoxides and 1,2-epoxides were characterized by PXRD. Figure 7 contains the PXRD patterns of iron(III) oxide aerogels prepared with DMO, TMO, and PO. All three diffraction patterns contain weak broad peaks typical of poorly crystalline materials. The low intensity of the XRD peaks for these materials may also be compounded by the extremely porous nature of the

(18) Poco, J. P.; Satcher, J. H., Jr.; Hrubesh, L. W. *J. Non-Cryst. Solids* **2001**, *285*, 57.

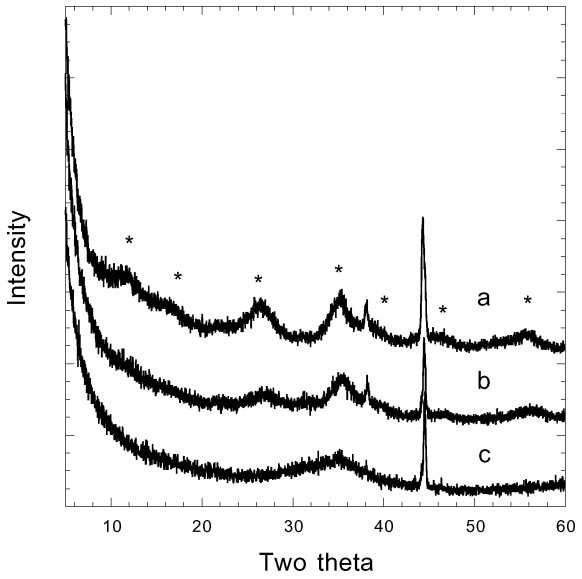

Figure 7. Powder X-ray diffraction patterns of iron(III) oxide aerogels prepared with (a) DMO, (b) TMO, and (c) PO. Note that the sharp peaks at 38° and 44° are due to the aluminum sample holder.

samples. Notwithstanding, some of the PXRD patterns contain discernible peaks that can be indexed. The iron(III) oxide aerogels made with DMO and TMO (Figure 7a,b) have several distinct peaks in common. When indexed, these peaks correspond to those for β-FeOOH, akaganeite (JCPDS file, 34-1266). Peaks present in both PXRD patterns at 2θ values of 11.8°, 16.8°, 26.7°, 35.2°, 39.2°, 46.4°, and 55.9° are marked with asterisks in Figure 7 and match those for akaganeite very well. The PXRD pattern for the iron(III) oxide aerogel (Figure 7c) made with PO only contains one broad peak that could not be indexed and assigned to any known iron(III) oxide phase. Ongoing studies elsewhere have shown that PXRD patterns from iron(III) oxide gels derived from $FeCl_3 \cdot 6H_2O$ with propylene oxide match those for the two-line ferrihydrite phase.[19] This phase, typically exhibits very poor crystallinity.[2,3]

Nitrogen Adsorption/Desorption Analysis. Aerogels are compliant materials, and in some cases, the pore volume and sizes can be distorted as N_2 condenses in the pores and capillary pressure is exerted on the material. There have been several recent publications describing erroneous pore size distribution and pore volume measurements of aerogels using gas adsorption techniques and methods to obtain more accurate data.[20−23] By allowing longer equilibration times during data collection, these problems can be eliminated. We acknowledge this and have modified our data collection parameters (see Experimental Section) to mitigate any such problems. Therefore, we have strong confidence that the results presented here are accurate and representative of the aerogel material.

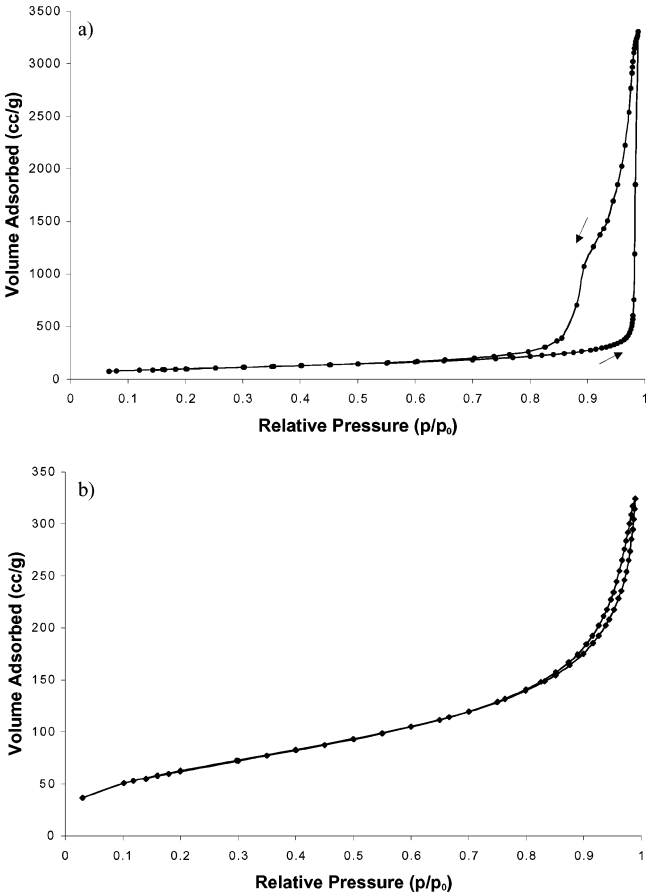

Figure 8. (a) Isotherm for β-FeOOH made using TMO and (b) isotherm for β-FeOOH made using DMO.

The nitrogen adsorption/desorption results for the iron(III) oxide aerogels are interesting. Table 2 contains a summary of the surface area, average pore diameter, and pore volume of the selected aerogels. All three materials have comparable and high surface areas. Several reports indicate that synthetic β-FeOOH has surface areas from 15 to 150 m^2/g.[24−27] The materials prepared here have specific surface areas significantly larger than that. There are marked differences in the average pore diameters and pore volumes for the aerogels reported here. Although the porosity of the DMO-derived aerogel is extremely high (∼99%), the measured pore volume is only 0.56 cm^3/g. By comparison, both the PO- and TMO-derived aerogels have much larger pore volumes, 3.88 and 5.93 cm^3/g, respectively. In addition, the average pore size of the DMO-derived aerogel is 8.1 nm, which is significantly smaller than the 31 and 23 nm values found for the TMO- and PO-derived aerogels.

Not surprisingly, there are also differences in the isotherms for the three aerogels. Figure 8 contains the isotherms for both the TMO- and DMO-derived aerogels. The isotherm for the DMO-derived aerogel is reversible type IIa and has essentially no hysteresis loop. Type IIa isotherms are typical of nonporous or macroporous

(19) Eggen, U. undergraduate thesis, University of Burgdorf, Switzerland, June 2002.
(20) Scherer, G. W. *J. Non-Cryst. Solids* **1998**, *225*, 192.
(21) Reichenauer, G.; Scherer, G. W. *J. Non-Cryst. Solids* **2000**, *277*, 162.
(22) Reichenauer, G.; Scherer, G. W. *J. Non-Cryst. Solids* **2001**, *285*, 167.
(23) Reichenauer, G.; Scherer, G. W. *J. Colloid Interfacial Sci.* **2000**, *236*, 385.
(24) Parida, K. M. *J. Mater. Sci. Lett.* **1987**, *6*, 1476.
(25) Parida, K. M. *J. Mater. Sci.***1988**, *23*, 1201.
(26) Naono, H.; Sonada, J.; Oka, K.; Hakuman, M. In *Fundamentals of Adsorption IV*; Suzuki, M., Ed.; Kodansha: Tokyo, 1993; p 467.
(27) Naono, H.; Fujiwara, R.; Sugioka, H.; Sumiya, K.; Yanazawa, H. *J. Colloid Interface Sci.* **1982**, *87*, 317.

solids and are normally associated with monolayer/multilayer adsorption on an open and stable surface.[28] The isotherms of the PO- and TMO-derived materials very much resemble those of type IIb and have significant hysteresis loops (especially the TMO-derived aerogel) best categorized as H3 or H4 loops. Hysteresis loops are associated with the filling and emptying of mesopores by the condensate. A major difference between the isotherms shown in Figure 8 is the total volume of gas adsorbed. A comparison of the isotherms indicates that much more nitrogen is adsorbed by the TMO-derived aerogel. This is reflected in the total pore volume values for the two solids. The microporosity of the DMO- and TMO-derived aerogels is relatively small and comparable. This is understandable as the fundamental building blocks, polycrystalline akaganeite, are the same in both samples and is consistent with previous studies that showed little to no microporosity of β-FeOOH.[26,27]

Discussion

We have reported on the use of propylene oxide as a gelation agent for the synthesis of iron(III) oxide aerogels and xerogels from Fe(III) inorganic salt precursors.[12,13] A mechanistic study, using pH measurements and NMR, revealed that the added epoxide acts as an irreversible proton scavenger that induces the Fe(III) species to undergo hydrolysis and slow and uniform condensation to form an iron(III) oxide sol. This results in uniform pH gradients in solution, hence there are little variations in the hydrolyzed species that form, and leads to aerogels with reproducible characteristics. This approach circumvents many of the problems associated with common synthetic approaches to the iron(III) oxides (e.g., direct addition of strong base).[3] The epoxide acts as simple base by undergoing the reaction shown in reaction 1. In the iron(III) system the acidic species

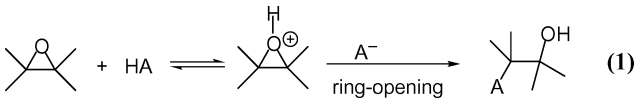

(1)

(HA) reacting with the epoxide is likely an Fe(III) aquo or aquo/hydroxy species and the anion is chloride. Undoubtedly the number and nature of the substituents on the epoxide used in reaction 1 strongly influence the kinetics of 1. Since this reaction is associated with the condensation of the Fe(III) monomers in the sol−gel polymerization, epoxide variation provides a way to try and direct the kinetics of sol particle growth and aggregation. Fine control of these parameters would allow more control of the microstructure and, thus, the properties of the resulting gel.

The nucleation and growth of akaganeite is known to occur at low pH.[2,3] The pH is one of if not the most important factor in akaganeite synthesis. Cai et al. recently demonstrated that akaganeite is reliably prepared when the pH of $FeCl_3$ solutions is $\leq\sim 2$ before microwave heating. At higher pHs, other products begin to be formed with hematite dominating at pHs of ≥ 6.[29] The low pH slows down hydrolysis of $FeCl_3$ solutions and leads to akaganeite formation. Higher pH speeds up the hydrolysis of $FeCl_3$ solutions and leads to the formation of amorphous iron oxide, α-FeOOH (goethite), and α-Fe_2O_3.

The structure and substitution on the epoxide dictates its reactivity and, thus, affords some control over the rate of pH change, under a given set of conditions, and leads to the difference in aerogel morphology observed here. With the more reactive 1,2-epoxides the pH rise is rapid, and therefore, with addition of the full amount of epoxide, the solution is not at low pH for much time. These conditions do not favor the formation of akaganeite. It is likely that some small amount of β-FeOOH is formed using the 1,2-epoxides, but it is not prominent. This could account for the small amount of chloride 1−1.5 wt % seen in some samples. By comparison, when 1,3-epoxides are used, the pH rise is very slow, presumably due to the lower reactivity of the 1,3-epoxide. This allows significant nucleation and growth of iron(III) oxide sol particles at low pH with chloride present. These conditions are ideal for akaganeite formation and, thus, favor it when 1,3-epoxides are used. The 1,3-epoxides provide a simple and convenient way to prepare β-FeOOH in a one-step method.

To more thoroughly test this hypothesis, we prepared an iron(III) oxide gel monolith by slowly titrating an ethanol solution of $FeCl_3$ with propylene oxide. Incremental amounts of propylene oxide were added to the solution over the course of 20 h at room temperature before gelation occurred. Characterization of that dried gel revealed it to be β-FeOOH. Therefore, it seems that the rate of pH change is a key parameter in dictating the iron(III) oxide phase favored. According to Schwetmann and Cornell, once the pH rises to a critical value, growth of the amorphous iron(III) oxide phase from polynuclear iron(III) aquo and hydroxy aquo species is favored over that of crystalline FeOOH.[3]

When 1,2-epoxides are added in one step, the pH change is so rapid that little β-FeOOH is formed as an amorphous iron(III) oxide phase, likely ferrihydrite, is favored. Ferrihydrite is a poorly crystalline phase of hydrated iron(III) oxide and is often referred to as amorphous. Ferrihydrite is often the first precipitate formed by the hydrolysis of Fe^{3+}. It is prepared by the rapid hydrolysis of Fe(III) solutions by heating or rapid pH increase through the addition of strong base.[2,3] It is difficult to detect via PXRD using Cu Kα X-rays, and recent work suggests that it is the predominant phase when PO is used.[2,19] Given all of these factors, there is a strong probability that the PO-derived aerogel is ferrihydrite.

There are eight major iron oxide and hydroxyoxide phases known. All of these phases can be prepared via solution methods. It is well known that factors such as initial pH, Fe/OH ratio, and temperature are crucial to the formation of a desired phase. We recognize that the method described here may be a potential route to a variety of different iron(III) oxide-based aerogel materials. For instance, simply altering the initial pH of the Fe(III) solution with an acid, base, or buffer before epoxide addition may enable the synthesis of alternative iron(III) oxide aerogels.

(28) Rouquerol, F.; Rouquerol, J.; Sing, K. *Adsorption by Powders and Porous Solids*; Academic Press: San Diego, 1999.

(29) Cai, J.; Liu, J.; Gao, Z.; Navrotsky, A.; Suib, S. L. *Chem. Mater.* **2001**, *13*, 4595.

he nitrogen adsorption/desorption results for iron(III) oxide aerogels are interesting. Although the porosity of the DMO-derived aerogel is extremely high (~99%), the measured pore volume is low when compared to that for the PO- and TMO-derived aerogels (see Table 2). This implies that the DMO-derived material has considerably less mesopore volume than the PO- and TMO-derived aerogels and that its pore volume must be dominated by macropores (i.e., those larger than 50 nm). Macropores are not filled by condensed nitrogen in this type of analysis.[28] Therefore, they are not factored into pore size or volume analyses. This explains the lower pore volume and average pore size values for the DMO-derived aerogel relative to the TMO- and PO-derived aerogels. Thus, this synthetic approach to β-FeOOH provides considerable control over the amount of meso- and macroporosity in the resulting material.

One may ask why the pore volume and average pore size for the TMO- and DMO-derived aerogels are so dissimilar given the similarity of their respective microstructures. The microstructure of the DMO-derived aerogel is coarser than that of the TMO material (compare Figures 3 and 4). The constituent fibers of the TMO material have diameters that are nominally 2−5 nm, whereas those for the DMO aerogel look to be significantly thicker, in the 15−35-nm range. It is this difference that accounts for the abundance of mesoporosity in the TMO solid and the lack of it in the DMO solid. The size difference, of the constituent fibers, may be a result of the slower growth of the DMO material at low pH when compared to the TMO material. The slow growth of the DMO material is likely related to the lower reactivity of the DMO to nucleophiles, when compared to the TMO.

Aerogels display very interesting mechanical and acoustical properties. For example, SiO_2 aerogels have been shown to transmit sound velocity waves at speeds below that of any other inorganic solid measured.[11] This unique property may allow them to be used in sound insulation or acoustical delay line applications. Acoustical measurements of sound velocity were used to evaluate the mechanical properties of some selected iron(III) oxide aerogels made via epoxide addition.

Comparisons of the elastic moduli of the β-FeOOH aerogel materials made here to those for reported elsewhere for silica and alumina aerogels, of the same density, are very favorable.[16] From Table 2 it can be seen that the akaganeite aerogels are measurably stiffer than the silica and alumina ones. This is significant as both silica and alumina have often been thought of as prime examples of rigid aerogel materials.[9] The akaganeite aerogels can be easily handled and even machined with few handling restrictions. This stiffness also allows β-FeOOH aerogels to be sintered to monolithic α-Fe_2O_3 (hematite) aerogels (~85% porous). Even with the considerable volume reduction (aerogel density increases from 40 to 770 kg/m^3), the monolith does not shatter. To our knowledge, this is the first report of aerogel monoliths of hematite.

The higher strength of the 1,3-epoxide-derived aerogels compared to 1,2-epoxide-derived ones is likely due to the greater interconnectivity of their respective microstructures. For a given density, the elastic modulus (stiffness) of an aerogel can be up to 1 order of magnitude higher due to increased connectivity of the microstructure.[30] The slow gel times of the 1,3-epoxides favor the formation of a highly reticulated microstructure that is responsible for the stiffer character of the resulting aerogel. Several reports have modeled the microstructure of sol−gel materials and how it relates to the mechanical properties of the gel.[30,31]

The elastic modulus of an aerogel depends on the connectivity of the constituent particles in space. Every particle in the network is connected to one or more other particles. Those connected to one other particle are termed “dead ends”; those connected to more than one other particle are part of a loop. The “dead end” particles do not help the overall macrostructure bear any load, whereas the particles in “loops” do contribute to the load bearing of the overall macrostructure. A microstructure with a preponderance of “dead ends” is mechanically inefficient when compared to one with less.[31] The slow nucleation and growth of the β-FeOOH particles via the epoxide addition method leads to a minimization of the surface energy of the particles and the minimization of “dead ends”. This leads to a more completely connected network and greater mechanical integrity of the resulting aerogel.

In summary, a new straightforward room-temperature approach to akaganeite aerogels is reported. Stiff monolithic aerogels with controllable levels of meso- and macroporosity are readily prepared with 1,3-epoxides.

Acknowledgment. This work was performed under the auspices of the U.S. Department of Energy by the University of California, Lawrence Livermore National Laboratory under Contract W-7405-Eng-48. Special thanks go to Dr. Jurgen Plitzko for TEM analysis, Mr. Jim Ferreira for SEM analysis, Dr. Cheng Saw for PXRD measurements, and Mr. Ing Chiu for thermal analysis.

CM034211P

(30) Woignier, T.; Reynes, J.; Hafidi Alaoui, A.; Beurroies, I.; Phalippou, J. *J. Non-Cryst. Solids* **1998**, *241*, 45.

(31) Ma, H.-S.; Prévost, J.-H.; Jullien, R.; Scherer, G. W. *J. Non-Cryst. Solids* **2001**, *285*, 216.